FATIGUE DAMAGE MECHANISM AND ITS APPLICATION BASED ON FULL-SCALE ANALYSIS OF STEEL-CONCRETE COMPOSITE SLAB SUBJECTED TO REPETITION OF TRAFFIC

Yotaro OGIYAMA*, Chikako FUJIYAMA**, Takehiro TAKASUKA, Toshio MATSUMURA

Graduate School of Civil and Environmental Engineering, Hosei University, Japan *

Associate Professor of Civil and Environmental Engineering, Hosei University, Japan **

Japan Bridge Association, Japan***

ABSTRACT: The purpose of this study is to analyze the fatigue damage process of a plate girder bridge supporting a steel-concrete composite slab, and to propose a method for maintenance of the composite slab. To analyze a full-scale bridge subjected to heavy traffic, three-dimensional non-linear FE analyses and loading rates based on an actual bridge are used.

The full-scale bridge model is a 2-lane road bridge with 30 m span length and 10.55 m width, consisting of main girders with vertical stiffeners, cross beams, and composite slab. All structural elements were modeled as solid elements in order to enable detailed examination of stress distributions, although shear studs throughout the bottom plate were implicitly modeled as interface elements. The initial bond and surface friction between transverse ribs and concrete were taken to be the other types of interface elements.

First, a static load was applied to the center of the slab at the mid-span of the bridge. Although slips between transverse ribs and concrete were observed during the static loading process, a rapid decrease of load carrying capacity of the composite slab was not observed.

Next, four parallel moving loads, simulating the loads of vehicles, were applied to the slab along the bridge axis. Under high cycle load repetition, development of strains around the ribs was observed. This indicates the characteristic cracking mechanism of concrete in the composite slab. Visualization of analysis enabled the clarification of the fatigue damage mechanism of the composite slab. This study indicates that inspection of this type of composite slab is important for road maintenance.

KEYWORDS: Composite Slab of Robinson Type, Fatigue Damage Analysis, Full Scale Analysis

1. INTRODUCTION

Steel-concrete composite slabs have been widely used in Japan (Japan Bridge Association 2008). Composite slabs generally consist of a concrete slab, a bottom steel plate, and shear connectors. Various types of shear connectors have been proposed, and the load carrying mechanisms of various types of composite slabs have been investigated by Fujiyama et al (2010, 2011) and Matsumura et al (2012).

One of the composite slabs studied in this paper is called "Robinson type". Shear studs and ribs are welded onto the bottom plate. The ribs primarily function to stiffen the bottom plate during concrete casting. The performance of "Robinson type" composite slabs have been examined both through experiment and three-dimensional FE analysis by

Kaido et al. (2004), though slab dimension was limited due to loading machine capacity limitations.

The purpose of this study is to analyze the failure mechanism of "Robinson type" composite slabs under fatigue load conditions of actual road bridges: deformations of main girders and cross beams, location of loading lanes, and speed of wheel running. It is hard to examine the effects of these conditions in experiment. Therefore, in this study, a bridge model based on the dimensions of the actual bridge in question was built for FE analysis. The large number of shear studs on the full-scale bridge model was converted to an interface element, which expresses equivalent elasticity of shear studs.

Two static analyses with different load positions and three fatigue analyses with various moving load intensities were conducted. The generation of cracks inside concrete was clarified in each analysis to explore the failure mechanism of the composite slab. This study enabled us to propose an inspection method to find critical cracks inside composite slabs.

2. BUILDING A FULL-SCALE MODEL
2.1 Analysis target – Full-scale bridge

The full-scale bridge model is a 2-lane road bridge with 30 m span length and 10.55 m width, consisting of main girders with vertical stiffeners, cross beams, and composite slab, as shown in Fig. 1. The composite slab and main structure were modeled as solid elements to examine details of stress distributions in the thickness direction, as shown in Fig. 2.

Thickness of the main girder was constant in the longitudinal direction, assuming a 30 mm upper flange, 33 mm lower flange, and 27 mm web. Thickness of the composite slab was 260 mm (steel bottom plate and concrete was 8 mm and 252 mm,
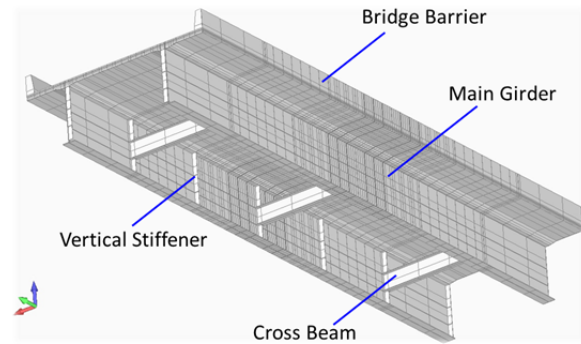

Fig. 1 General View of
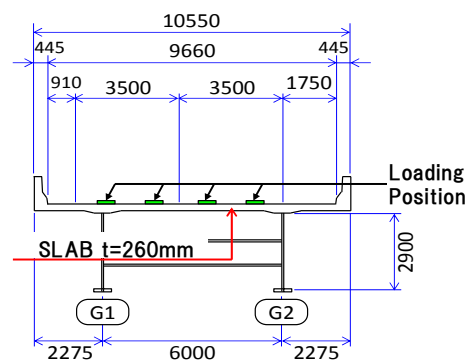Full-Scale Bridge Model

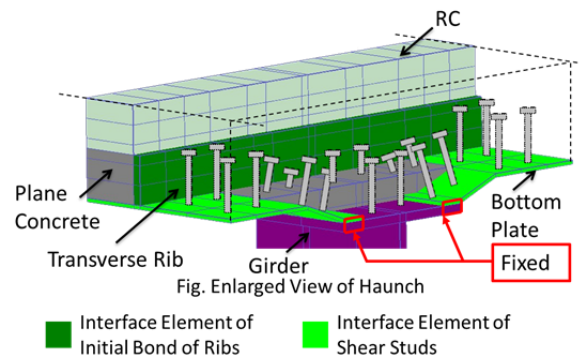

Fig. 2 Cross Section of
Full-Scale Bridge Model

Fig. 3 Arrangement of Interface Element

Tab. 1 Properties of Interface Element

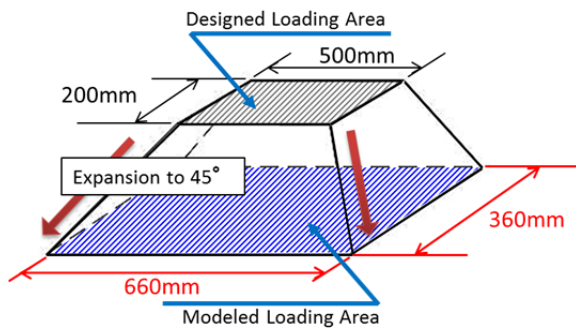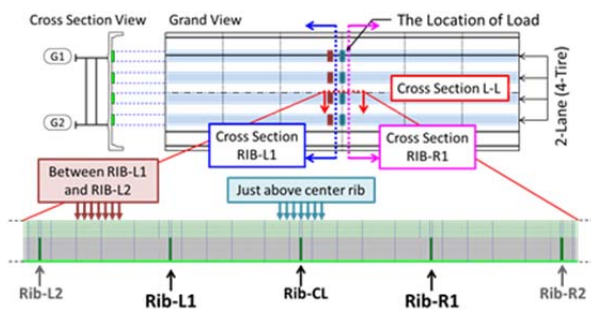| Properties	Studs, Bottom Plate	Rib
Shear Stiffness in Closure Mode(N/mm2)	11666	76923
Open Stiffness in Closure Mode(N/mm2)	28000	200000
Shear Stiffness in Open Mode(N/mm2)	22	1.5
Normal Stiffness in Open Mode(N/mm2)	37	1.5
Initial Bond (Shear) (N/mm2)	3.0	3.0
Initial Bond (Normal) (N/mm2)	3.0	3.0
Frictional Coefficient	99	0.6

Fig. 4 Mesh Generaton of Loading Area

Fig. 5 The Location of Load and
Focused Cross Section

respectively). In addition, the stiffness of the safety fence was considered by modeling the safety fence to reproduce behavior of the actual bridge, as shown in Fig. 1.

Longitudinal rebar D22 and transverse rebar D19 were expressed by steel ratio in an RC element, as in the preliminary analysis. The total number of nodes was 97,305 and the total number of elements was 81,467 (solid: 66,054, interface: 15,413).

The compressive strength and tensile strength of the concrete were 30.0 N/mm^2 and 2.2 N/mm^2, respectively. The yield strength of the transverse ribs and the bottom steel plates were 345.0 N/mm^2. Both ends of the main girders were restrained in the vertical direction at the lower flange to reproduce a simple support condition, as shown in Fig. 2.

2.2 Modeling of interface element
In general, modeling of a shear connector is

important for a composite slab. Modeling the shape of the studs is not realistic because "Robinson type" composite slabs have a large number of studs. Thus, the model is simplified in this study by using an interface element, which expresses equivalent elasticity of shear studs throughout the steel bottom plate. Furthermore, the initial bond and surface friction between steel and concrete were considered as another interface element.

Interface elements are organized for two surfaces (see Fig. 3). One is prepared for the surface of the bottom plate to consider the elasticity of the studs. Another one is prepared for the surface of the transverse ribs to consider the initial bond and friction between steel and concrete.

The equivalent elasticity was determined by considering the total number of studs. Before separating the bottom plate and the concrete, the normal and shear stiffness of the interface element was defined to be the same as the stiffness of the concrete. Once the gap occurred between the two, the stiffness of the interface element became based on the studs.

The rupture of the studs was not considered in this model because the studs kept their stiffness throughout the entire loading process (Kaido et al., 2004). The initial bond and surface friction of the interface element for rib surface were estimated by Rabbat, B. G. and Russell, H. G (1985). Details of these properties are shown in Tab. 1.

2.3 Constitutive Laws
The constitutive laws of plain concrete and reinforced concrete used herein consist of three basic yet essential models that are: compression, tension, and crack shear models. This can simulate nonlinear behavior of 3D concrete by tracing the evolution of

microscopic material states at each moment (Maekawa et al 2003). In terms of the constitutive law of steel, a general bi-linear model was adopted.

3. STATIC ANALYSIS OF FULL-SCALE MODEL

3.1 Loading condition

Four parallel loading areas were prepared as the full-scale model is a 2-lane (4-tire) road bridge. The spacing of the areas was set based on Specifications for Highway Bridges in Japan (1996). The dimension of each area is 360 mm x 660 mm because the distribution of load due to the thickness of pavement was considered by mesh generation (see Fig. 4). Nodal forces were directly applied to all the nodes in the area step by step from 50 kN to 1000 kN per one unit of area. In order to observe the different stress distributions inside the concrete, two load conditions were organized for static analyses. The first one set the four parallel loading areas above the center of the rib. The second one set them between Rib-R1 and Rib-R2, as shown in Fig. 5.

3.2 Results of analyses

3.2.1 Crack generation in slab

In order to generate cracks inside the concrete, particular focus was given to the strain distributions of the composite slab. The criterion of cracking was generally considered to be about 200 μ of strain.

The location of the loading area at this moment is shown in the cross sectional view at the mid-span in Fig. 5. The main frame seems to be slightly deformed, however, the influence on the deformation of the composite slab might not be dominant. Fig. 6 shows contour maps of vertical strain of the composite slab in the cross section L-L at the loading area above the center rib. The band of high strain area can be observed just below the loading area.
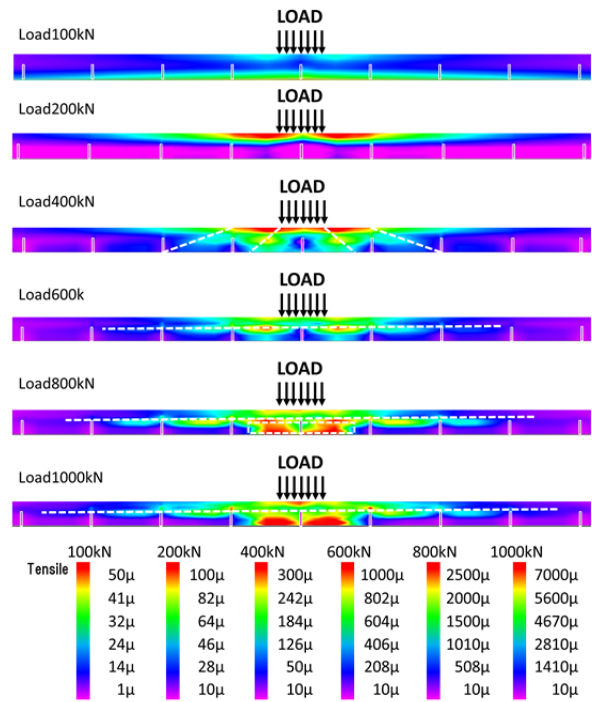

Fig. 6 Contour Maps of Vertical Strain in Cross Section L-L During Loading Above the Center Rib
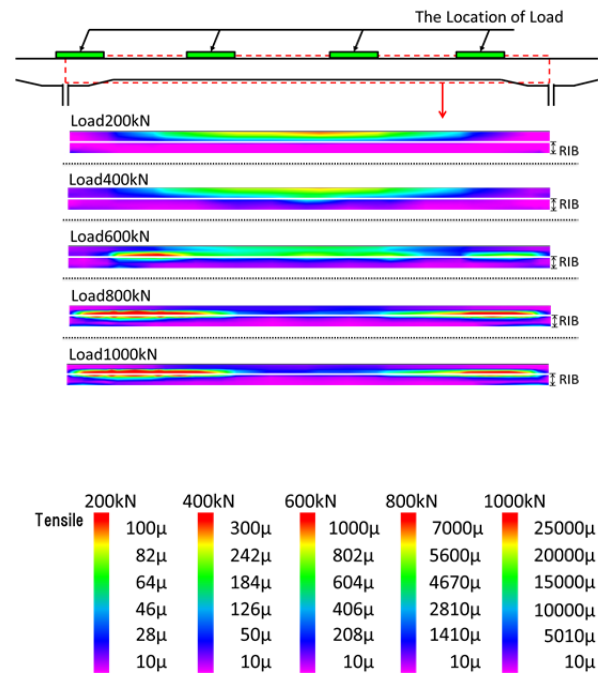

Fig. 7 Contour Maps of Vertical Strain In Cross Section Rib-R1

This indicates that the horizontal cracks occurred here and linked together through the tips of the ribs. Consequently, these generations of horizontal cracks might lead to the separation of the concrete slab. Another diagonal band of high strain area can be

seen between Rib-L1 and Rib-L2, as well as between Rib-R1 and Rib-R2 at load 400 kN per one unit of area. However, the direction of dominant stain bands changed from diagonal to horizontal when the load reached 600 kN.

Fig. 7 shows contour maps of vertical strain in the cross sectional direction at Rib-R1. For this load condition, the high strain band, considered as horizontal cracks in the transverse direction, appeared at a load 600 kN.

Fig. 8 is an assortment of contour maps of vertical strain in cross section of L-L when the location of the load was shifted from above the center rib to between Rib-L1 and Rib-L2. Similar strain distributions are observed in Fig. 6. However, diagonal cracks are not observed.
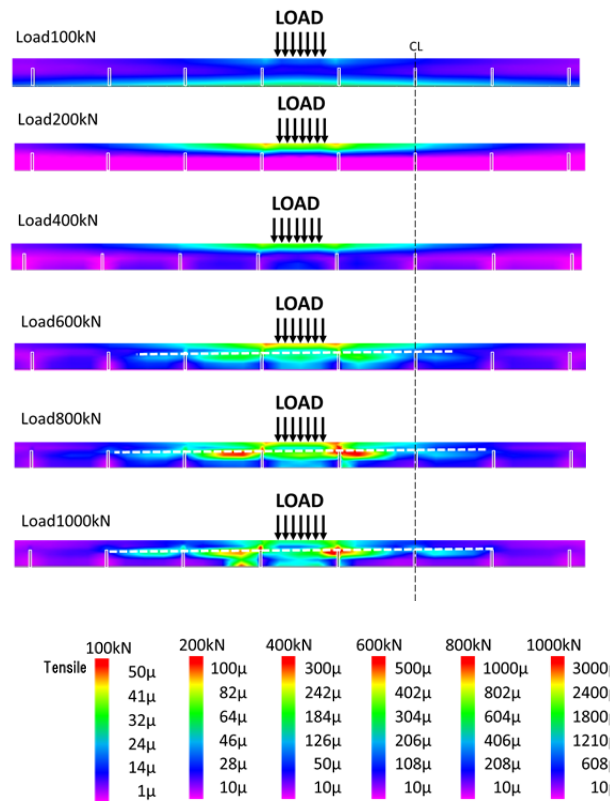
3.2.2 Damage mechanism under a static load

On the basis of the strain distributions inside concrete, as shown in Fig. 6-8, cracks were generally initiated from the tip of the ribs that locate near the loading area when the load reached 600 kN per 1 wheel (six times the design load). These cracks developed in the horizontal or diagonal direction, depending on the location of the load.

However, when the load increased, cracks progressed horizontally regardless of the location of the load, and they linked with neighbors. Consequently, the composite slab was separated into two layers by the horizontal cracks. We name this "2 layered" failure.

4. FATIGUE ANALYSIS OF FULL-SCALE MODEL

4.1 Loading conditions

To reproduce the load condition of a 2-lane (4-tire) road bridge, parallel 4-area loads were applied to the

Fig. 8 Contour Maps of Vertical strain
In Cross Section L-L
During Loading Between Rib-R1 and Rib-R2

full-scale model from the right end to the left end, as shown in Fig. 9. Each loading area was 360 mm × 660 mm, the as same as in the static analysis. The speed of the moving load was set to 100 km per hour based on Government Order on Road Design Standards (1970) in Japan, Type 1 Class 2. The magnitude of loads was 100 kN per 1 wheel, based on Specifications for Highway Bridges (1996) in Japan.

This is the prototype load condition, CASE A. In addition, the performances under 300 kN (three times the design load) and 500 kN (five times the design load) per 1 wheel were examined in order to consider the damage mechanism under excessive loads. They are named CASE B and CASE C, respectively.

4.2 Results of analysis

4.2.1 Number of cycles – deflection of slab

Fig. 10 shows the deformations of the full-scale model when the loads passed points (A)-(E). It shows the proper deformations of the slab with the movement of the loads. Since the continuity of slab was eliminated in the model, the greatest deflections occurred when the loads were located at the ends of the slab.

Fig. 11 shows the progress of maximum deflection at the bottom plate at mid-span with increasing number of load passages. Any recognizable increases of maximum deflections with the increase of the number of load passages were not observed for CASE A and CASE B. This indicates that there might be slight damage progress in the composite slab under the repetition of design load. However, maximum deflection increased about 2 mm in CASE C. Therefore, we focused on CASE C to discuss the failure mechanism under moving loads.

Fig. 12 shows the vertical displacements of the main girder and slab at mid-span for CASE C. The vertical displacements were picked up at the lower flange of the main girders and that of the bottom plate of the slab. Although the displacement of the girder was constant, the displacement of the slab increased about 2 mm. This indicates that only the stiffness of slab concrete decreased step by step due to repeated loads; nevertheless, rapid increase of deflection caused by punching shear failure was not observed.

4.2.2 Crack generation in slab concrete

(a) Cross section of longitudinal direction after load passing through

There might be a change of strain distribution inside concrete, even if significant increasing of deflection
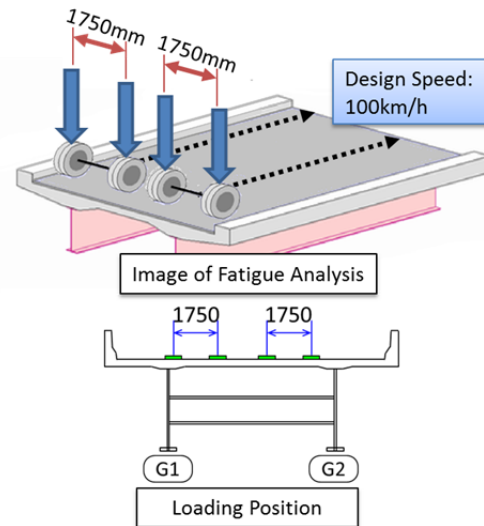

Fig. 9 Image of Fatigue Analysis
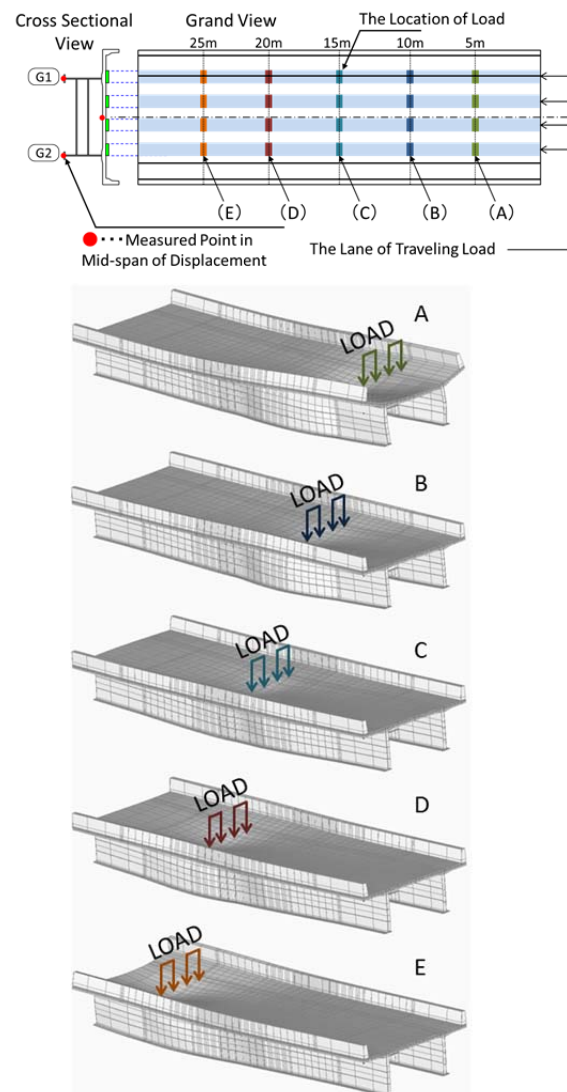and the Loading Position

Fig. 10 Magnified Deformation
During Traveling Load

of slab does not appear, as in CASE A and CASE B. First, a cross section along longitudinal direction was examined.

Fig. 13 shows contour maps of vertical stain at cross section L-L at number of load passage 10,000,000. A localization of tensile strain of about 50 μ was recognized around the Rib-CL in CASE A. However, there was no concentration of strain around the other ribs. Local strain concentration does not imply any serious damage of slab concrete at this moment. However, relatively high vertical strain appeared continuously from the tip of Rib-CL to the tip of Rib-R1 and Rib-L1 in CASE B. The strains in the band were about 150 μ, which approach the criteria for cracking. The local strains possibly had increased gradually in 10,000,000 cycles and almost reached the occurrence of horizontal crack in CASE B.

The situation of CASE C was very different from those of CASE A and CASE B. High vertical strain area of about 4000~6000 μ was observed in concrete around the tips of all ribs in CASE C. This indicates that horizontal cracks have already occurred from the tips of the ribs. Furthermore, the horizontal cracks linked with the tips of neighbor ribs. The link of horizontal cracks separated the concrete slab into two layers. Consequently, "2 layered failure" was seen in CASE C as well as static analysis.

For further analysis of the failure mechanism under the repetition of a moving load, the contour maps of vertical strain at number of cycles 10,000 and 1,000,000 are shown in Fig. 14. The specific area of vertical strain had been seen around the ribs at number of cycles 10,000. It glowed and generated horizontal cracks. After the large number of load passages, clear bands of high strain area
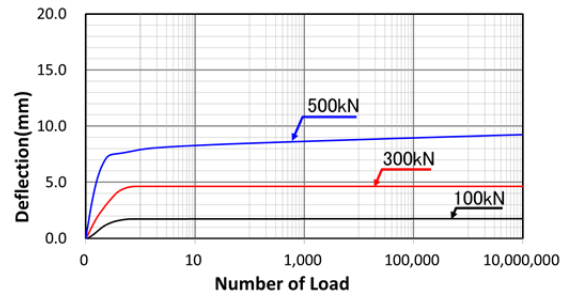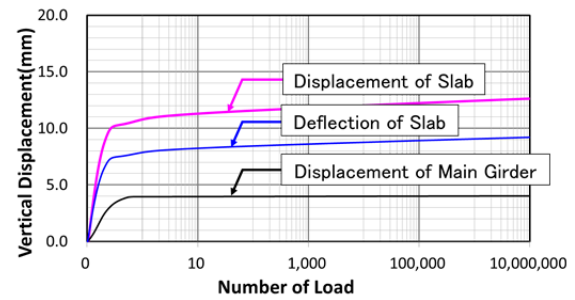

Fig.11 Deflection－Number of Load
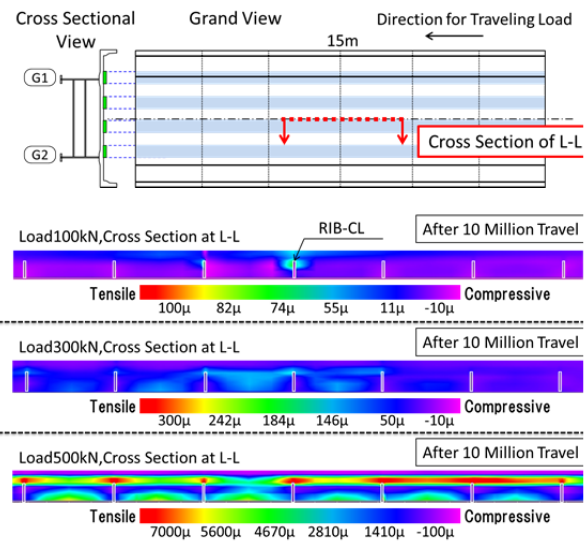

Fig.12 Vertical Displacement－
Number of Load

Fig. 13 Contour Maps of Vertical Strain
at Cross Section L-L at the Number of Load
Passage 10,000,000 (CASE AtoC)

could be observed in the horizontal direction in wide area at number of cycles 1,000,000.

The horizontal cracks confidently lead the separation of the concrete slab into upper and lower

layers. This suggests that "2 layered failure" occurred only when the high cycle repetition of excessive load came onto the composite slab.

(b) Cross section of transverse direction after load passing through

The strain distribution at the cross section in the transverse direction was studied for CASE C. Fig. 15 shows a contour map of maximum principal strain of the cross section of Rib-R1, Rib-R2 and Rib-R3 at number of cycles 10,000. The High strain band, about 500 μ, was observed just below the loading area at the mid-span. This indicates that the top of the slab concrete was damaged by direct loading. Maximum principal strain was seen above Rib-R1. The trend was clear near the center of the mid-span (in the order of Rib-R1, Rib-R2, Rib-R3). According to this study, a following process of crack generation in the transverse direction was deduced. First, concrete cracks occur from the tips of ribs close to the mid-span in the longitudinal direction. Second, the cracks develop to the neighbor ribs in the longitudinal direction. Then, the cracked area is widened in the transverse direction.

(c) Cross section of longitudinal direction focused on loading position

Next, we focused on the transition of concrete strain distribution by moving loads in order to consider the relation between loading position and behavior of concrete cracks. Figs 16-18 show contour maps of vertical strain at the cross section of longitudinal direction around number of cycles 10,000,000 for all cases.

Although slight transition of vertical strain was observed just below the loading area in CASE A and CASE B (Figs. 16 and 17), a specific concentration of vertical strain did not appear.
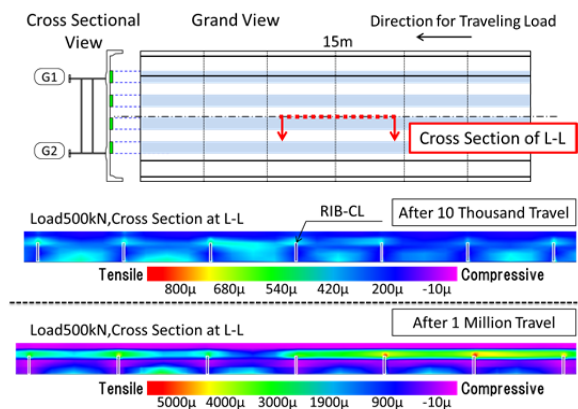

Fig.14 Contour Maps of Vertical Strain at Cross Section L-L at Number of Cycle 10,000 and 1,000,000 (CASE C)
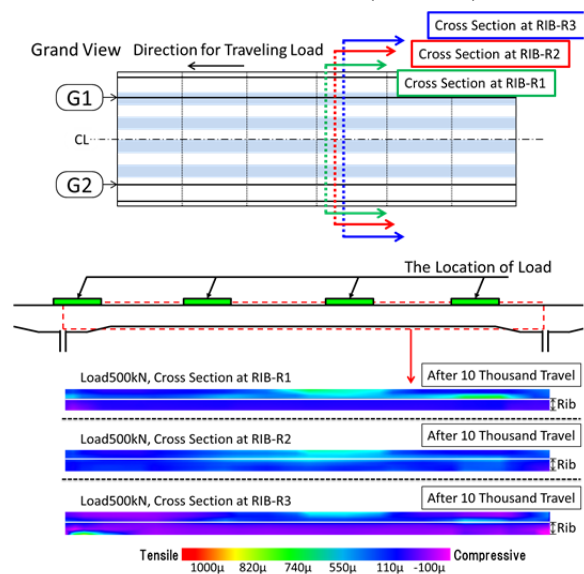

Fig. 15 Contour Maps of Maximum Principal Strain at Cross Section RIBs at Number of Cycle 10,000 (CASE C)

In contrast, vertical strain bands were clearly seen and grew in the horizontal direction with traveling load in CASE C, as shown in Fig. 18. The most highlighted vertical strain area were located in both sides of each load positions (A) to (E). Then, even after the load passage, the residual strains about 500μ, which means cracked element, were recorded continuously in horizontal direction at the load position (B) to (E).

On the basis of the above-mentioned study, it can be said that load travelling affects horizontal crack generation in the composite slab.
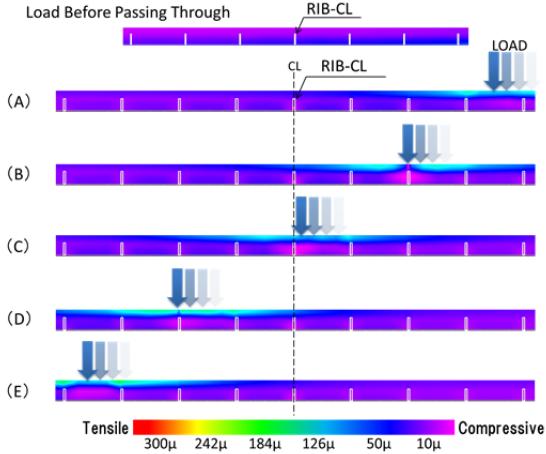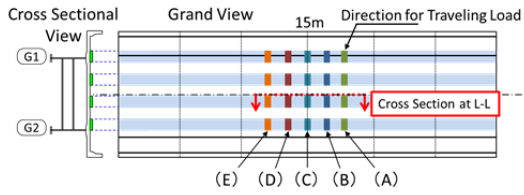
Fig.16 Contour Maps of Vertical Strain
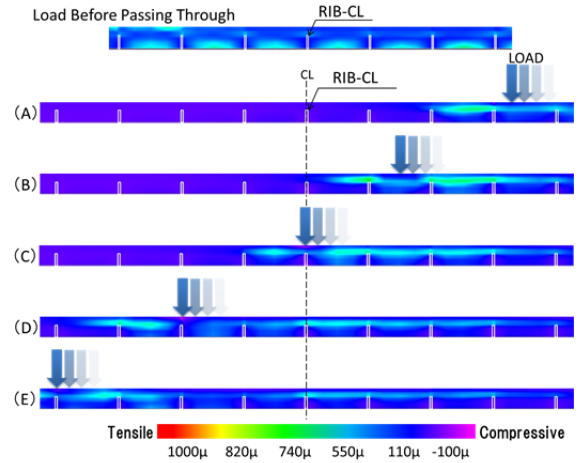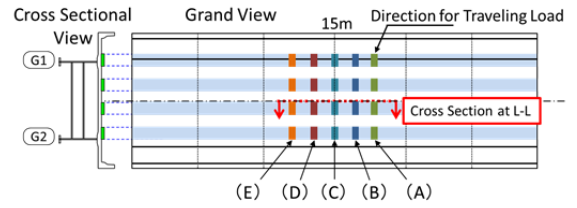At Cross Section L-L in 100kN (CASE A)

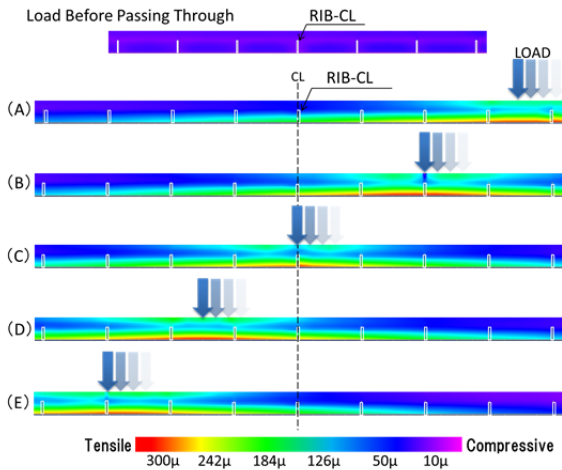Fig. 17 Contour Maps of Vertical Strain
at Cross Section L-L in 300 kN (CASE B)

Fig. 18 Contour Maps of Vertical Strain
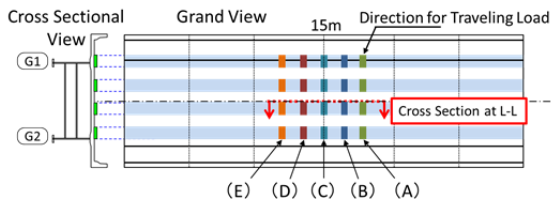at Cross Section L-L in 500 kN (CASE C)
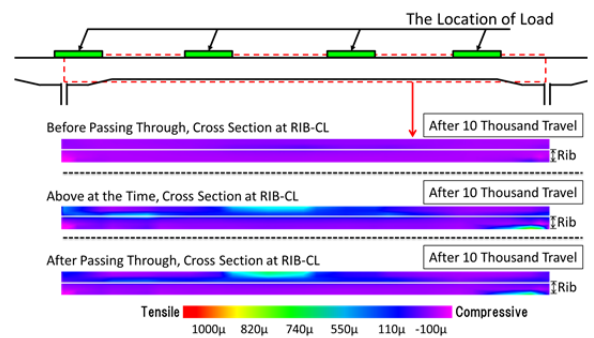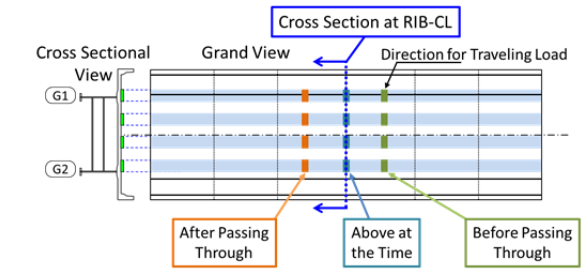
Fig. 19 Contour Maps of Vertical Strain
at Cross Section Rib-CL (CASE C)

(d) Cross section of transverse direction focused on loading position

The same study was further conducted in the transverse direction for the case of before, under, and after the passage of loads. Fig. 19 shows a contour map of vertical strain at cross section of Rib-CL at number of cycles around 10,000,000 in CASE C.

The vertical strain of the upper concrete element at the cross section of Rib-CL increased under the

passage of load set. After the passage, about 500 μ residual strain remained along the top of the rib. This indicates that the horizontal cracks were developed in the transverse direction along ribs under the passage of load set.

4.2.3 Damage mechanism under the fatigue load

On the basis of fatigue analysis reproducing the repetition of load travelling on the full-scale model assuming a 2-lane road bridge, the "two layered failure" mechanism of the composite slab was similar to that observed in the static analysis. The horizontal cracks occurred from the tips of ribs and linked together when an excessive load passed approximately more than 10,000 cycles. The horizontal cracks tended to grow up longitudinally when the loads passed above the ribs. Furthermore, the horizontal cracks spread in the transverse direction along each rib. Consequently, the horizontal cracks lead to the separation of the concrete slab. The mechanism was never seen under proper load intensity, even if the number of load repetitions reached 10,000,000 cycles.

5. INSPECTIONS BASED ON THE FAILURE MECHANISM

5.1 Possible inspections based on the failure mechanism

The static analyses and fatigue analyses in this study described two aspects of the failure process of the composite slab. First, critical damage: horizontal cracks occur and develop inside the slab concrete. Second, the composite gradually loses its stiffness due to the spread of the "two layered" area, but does not fail drastically. Therefore, to find the horizontal cracks at this early stage is most critical. The extra time to failure should be properly used for repairing to prolong the life of the composite slab.

In general, visual inspection of a composite slab is impossible because the top and bottom of the slab is covered by pavement or a steel bottom plate, respectively. As a matter of maintenance on the composite slab, non-destructive inspections, such as electromagnetic wave radar, thermography, and the elastic wave method, can be applied. In particular, thermography and the "shear wave resonating method" are recommended.

Thermography is a method that inspects temperature differences by using an infrared imaging device. The device records the infrared rays emitted from the object surface. Even though it cannot directly inspect the conditions inside concrete, the difference of surface temperature due to rock pockets or caves can be captured. This could be applicable to finding the spread area of horizontal cracks, especially after rain. Horizontal cracks supplemented with rainwater between concrete partially changes the specific heat of the composite slab. The location near the ribs should be carefully inspected based on the failure mechanism.

The shear wave resonating method inspects the discontinuity of solid material, like cracks, by measuring the vibration caused by a sonic shear wave including a low-frequency component. This method is now under development for detecting the water existing in the separation of the steel bottom plate and the concrete slab (Japan Bridge Association 2012). It is expected that the method will be utilized soon.

6. CONCLUSIONS

The full-scale model of a plate girder bridge supporting steel-concrete composite slab was investigated using three-dimensional non-linear FE analyses. The full-scale bridge model was built and both static and fatigue analyses were conducted to clarify the failure mechanism. On the basis of analysis, we propose possible non-destructive

inspection methods for the composite slab. The following are the salient conclusions:

1) Full-scale bridge model reproduced the behavior of the actual bridge.

2) A static load was applied to the model based on the actual road conditions of bridges.

3) The failure mechanism of the composite slab under the static load was clarified. First, horizontal cracks occurred from the tips of the ribs. Next, horizontal cracks linked to neighbor ribs. Finally, the composite slab was separated into two layers, called "2 layered failure".

4) On the basis of fatigue analysis reproducing the repetition of load travelling on the full-scale model assuming a 2-lane road bridge, the "2 layered failure" mechanism was similar to that observed in static analysis when an excessive load was applied. The mechanism was never seen under proper load intensity, even if the number of repetition of load reached 10,000,000 cycles.

5) The horizontal cracks tended to grow up longitudinally when the loads passed above the ribs. Furthermore, the horizontal cracks spread in the transverse direction along each rib. Consequently, the horizontal cracks lead to the separation of the concrete slab.

REFERENCES

C. Fujiyama and K. Maekawa,2011. A computational simulation for the damage mechanism of steel-concrete composite slabs under high cycle fatigue loads, *Journal of Advanced Concrete Technology*, Vol.9, No.2, pp.193-204, (In Japanese)

C. Fujiyama, F. Shang, N. Sakurai and K. Maekawa, 2010. Fatigue Life Simulation and Failure Mode for Stee-lconcrete Composite Bridge Deck Based upon a Direct Path-Integral Scheme, *Journal of JSCE*, Vol. 66, No. 1, pp.106-116, (In Japanese)

H. Kaido, H. Watanabe, Y. Tachibana, S. Matsui and T. Horikawa, 2004. Evaluation for fatigue durability of steel plate-concrete composite deck by wheel trucking test and three-dimensional finite element analysis, *Journal of Structural Engineering* Vol. 50A, pp. 1119-1130. (In Japanese)

Japan Bridge Association, 2008. Applying of composite slab - History of development・Current and future, *Bridge Technology Presentation Article*, pp.23-33. (In Japanese)

Japan Bridge Association, Subcommittee on Bridge Slab Engineering, 2012. For conservation technology of concrete bridge slab, *Bridge Technology presentation Article*. (In Japanese)

Japan Road Association, 1996. *Specifications for Highway Bridges: Common edition*, pp.9-16. (In Japanese)

Maekawa, K., Pimanmas, A. and Okamura, H., 2003. Nonlinear Mechanics of Reinforced Concrete, *Spon Press*, London.

Ministry of Land, Infrastructure, Transport and Tourism, 1970. Government Order on Road Design Standards,URL:

http://www.mlit.go.jp/road/sign/kouzourei_kaisetsu.html

Rabbat, B. G. and Russell, H. G.,1985. Friction coefficient of steel on concrete or grout, *Journal of Structural Engineering*, Vol.111, No.3, pp.505-515

T. Matsumura, A. Kamimura, C. Fujiyama and K. Maekawa, 2012. Fatigue damage simulation analyses on steel-concrete composite deck subjected to wheel running test loading, *The 7th Symposium of Road Bridge Slab*,pp.269-274. (In Japanese)